Chapter 5
Case Study 2.2: Clamping of Thin-Walled Curved Workpieces

Petr Kolar, Jiri Sveda and Jan Koubek

Abstract Thin-walled curved workpieces are typical for structural parts of airplanes. The issue in the workpiece clamping and subsequent machining is the changeable workpiece stiffness during material removal. The fixture forces and the cutting forces deform the workpiece with dependence on the part decreasing static stiffness that causes large local surface location errors of the part. As a result, the workpiece wall thickness is out of tolerance and consequently the part's weight is also out of tolerance. The proposed solution is based on new fixtures with integrated support and clamping function. The workpiece is clamped using a vacuum. A suitable thickness measurement sensor was integrated into the machine tool. The new fixture elements are autonomous and plug-and-produce ready, with integrated safety by monitoring the minimal workpiece clamping force. The fixture control enables fully automated operation using the specific control software. The machining process was optimized in terms of tool path strategy and cutting conditions to avoid chatter during machining and shorten the production time. The proposed manufacturing process leads to a shortening of the production time with the requested surface quality. The presented manufacturing procedure is beneficial from the productivity and cost point of view. A group of fixtures, including the necessary harness and control, offers a universal possibility for replacing a set of six specific fixtures designed as a mould with part negative shape.

P. Kolar (✉) · J. Sveda · J. Koubek
Research Center of Manufacturing Technology (RCMT), Czech Technical University in Prague, Prague, Czech Republic
e-mail: p.kolar@rcmt.cvut.cz

J. Sveda
e-mail: j.sveda@rcmt.cvut.cz

J. Koubek
e-mail: j.koubek@rcmt.cvut.cz

5.1   Introduction of the Case Study

This case study is focused on clamping and machining of thin-walled curved workpieces. Such type of workpieces is often used for airplane structures. The aluminium parts are typically machined from a block of material. In this case, typical machining operations are high material volume removal during roughing and finishing of straight or curved thin walls. If the thin-walled parts are made of composite, the typical operations are finishing using edge trimming and rivet hole boring. The issue in the workpiece clamping in both mentioned cases is the curved shape and the compliance of the final part. The fixture system should clamp the part tight but must not deform it. The fixture should also stiffen the part for improving machining productivity.

Machining of the thin-walled aluminium part from a block of material is described in this case study. The main requirement is machining of the part with a specified part weight tolerance. The main challenge is changeable workpiece stiffness during material removal. The fixture forces and the cutting forces deform the workpiece with dependence on the part decreasing static stiffness that causes large local surface location errors of the part. As a result, the workpiece wall thickness is out of tolerance and consequently the weight of the part is also out of tolerance. This causes weight changes of the airplane structure which are critical for the final airplane parameters.

This case study has two related topics. Firstly, the wall thickness deviation is related to the low static stiffness of the workpiece. Dedicated "mould-type" fixtures with the negative shape of the part for full-surface clamping using the vacuum are often used in industry [1]. The main disadvantages of this solution are the high price, dedicated use and still non-defined part position due to compliance of the vacuum field seals that does not ensure for 100% production of the requested wall thickness. Secondly, the machining productivity is limited by the low dynamic stiffness of the part. The chatter theory is known from 1960s [2, 3]. However, the workpiece stiffness is changing during machining, which makes the process control challenging. There are various approaches dealing with simulation of the stable
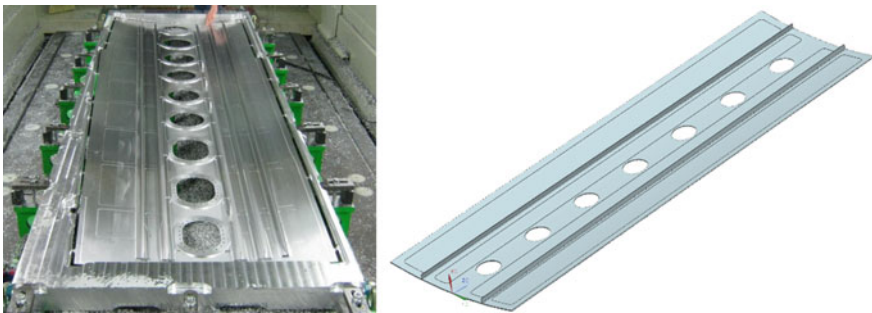

Fig. 5.1 The reference part for the case study (aluminium alloy 7075; outer dimensions: 1100 × 3000 mm; standard wall thickness: 2 mm; the margins have a thickness of 3 mm)

Table 5.1 Key performance indicators of the case study

| Parameter	Request	Previous technology
Workpiece wall thickness tolerance	±0.05 mm	±0.1 mm
Machining time of the inner side	to minimize	100 h
Workpiece weight tolerance	max. +1 kg	up to +2 kg
Surface roughness	Ra 0.8	Ra 0.8

machining limits and also surface roughness characteristic during thin-walled part machining [4–6].

The part used in this case study is a component of the wing of a "commuter" category airplane. The part main dimensions are presented in Fig. 5.1. The case study key performance indicators (KPIs) are presented in Table 5.1. The design request and previous production technology results are compared. As can be seen, the improvement of the wall thickness is the main goal of the case study.

The principle approach is based on the new fixture design supporting the workpiece in selected points, optimized machining strategy and adaptive machining technology involving the inspection of the current state of the workpiece geometry. The fixture and the thickness measurement sensor are connected with the machine tool control system. Specifically developed software is used for the control of the fixture clamping status and measurement procedures (path planning, measured data acquisition) using a touch probe and a thickness sensor. The machining technology was optimized to avoid chatter vibration and to minimize the cutting force that deforms the workpiece.

5.2 Demonstration Workpiece

For machining demonstration, a section of the whole real part was used for less expensive and less time-consuming proof-of-the-concept testing. Instead of downscaling the whole workpiece geometry, a section with outer dimensions of 1100 × 600 mm was used (Fig. 5.2).
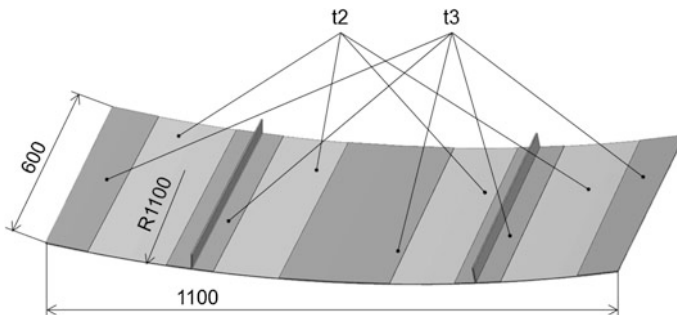
Fig. 5.2 CAD model of demonstration workpiece—a section of the airplane wing part
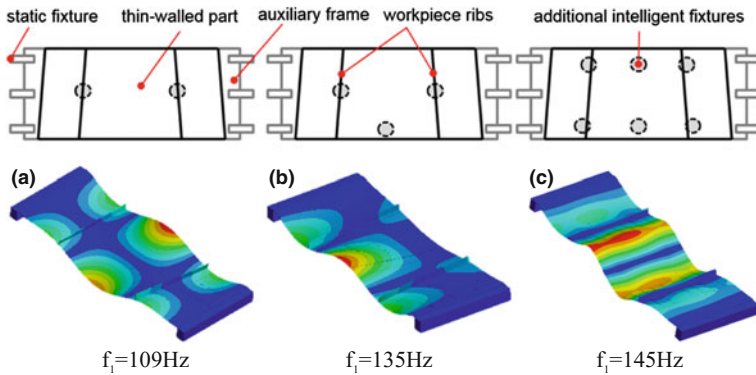
Fig. 5.3 Three clamping configurations: (a) with two additional fixtures; (b) with three additional fixtures; (c) with six additional fixtures. Workpiece first eigenvalues and related eigenmodes after clamping are shown

As FEM simulation in the free-free state confirmed, the modal behaviour of the demonstration workpiece is similar to the full-sized part. Thus, the short demonstration part can be used for testing of the whole technology. The results can be easily applied to the real part machining because the local dynamic behaviour of the workpiece with respect to the machining operation is similar.

The real full-sized part is clamped around the whole workpiece by an auxiliary frame. The thin wall is supported by a group of clamping and supporting points. The demonstration part behaviour (section of the full-sized part) was tested in four clamping situations: without additional fixture points and with three different fixture configurations. The auxiliary frame is applied only on two sides in case of the demonstration part (Fig. 5.3, top).

When analysing the workpiece first eigenmodes for the different clamping scenarios (Fig. 5.3), a high compliance of the workpiece central region in the case of two additional fixture points can be observed. Stiffening of the longer free edge with the third fixture brings partial improvement of the dynamic behaviour. The application of six fixtures gives small improvement of the static and dynamic workpiece properties. As can be seen, additional supporting points partially improve the workpiece stiffness and mainly influence the character of the eigenmodes. A significant part stiffening (e.g. increasing the frequency of the first eigenmode about factor 2 and more) is not possible if a limited number of supporting points is used. The large unsupported thin-walled area remains the main issue for machining.

The analysis of the static compliance of the finished and semi-finished workpiece with six supports was performed using FEA. The workpiece load by an axial cutting force was simulated by a force of 20 N. This force value was identified experimentally as usual finishing cutting force in normal direction to the machined surface. The static compliance graph and the total workpiece deformation is depicted in Fig. 5.4. As can be seen, the influence of the supporting points to the static stiffness is limited. A significant improvement is visible in the region of both
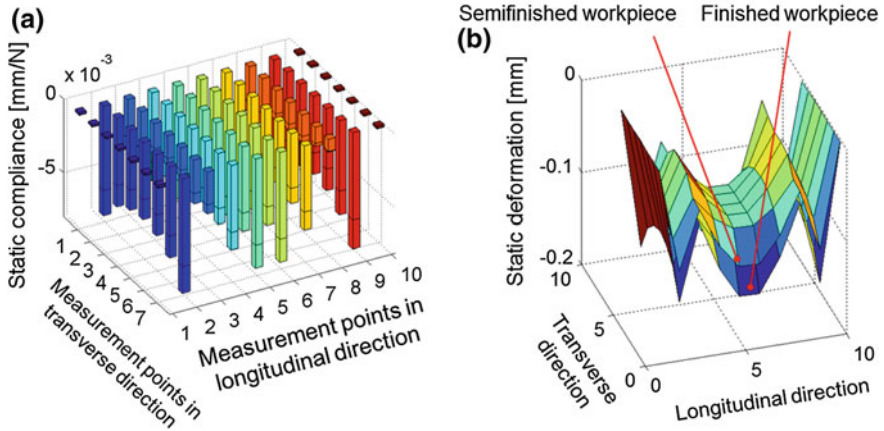
Fig. 5.4 FEA results of workpiece structural behaviour: (a) static compliance of finished and semi-finished workpiece; (b) comparison of workpiece static deformation due to axial cutting force

ribs only. The maximum value of the workpiece deformation is about 0.2 mm during machining. This deformation has to be compensated using a corrected tool path in order to stay within the requested part tolerance. The presented stiffness map is used for this operation, see Sect. 5.8.

5.3   Introduction of the Fixture Unit

The main functionality of the fixture unit is to set the specific height, lock this position and to clamp the workpiece. The main components of the developed fixture unit are shown in Fig. 5.5. The unit has a compact design. The piston rod is
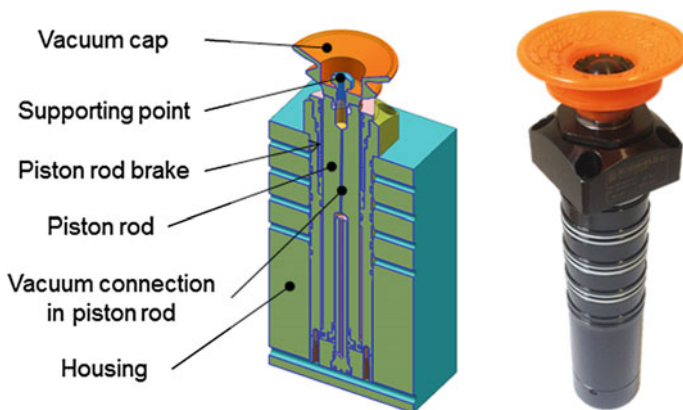

Fig. 5.5 The main components of the fixture unit

Table 5.2 Technical parameters of the fixture unit

Dimensional parameters: Minimum fixture height: 300 mm Piston rod stroke: 100 mm Piston rod diameter: 32 mm Vacuum cup diameter (changeable), starting from: 25 mm	
Hydraulic circuit parameters: Working pressure: 1.5–6.0 MPa Oil flow: 2.1 l/min Hose size: DN8 Positioning force range: 120–470 N	*Vacuum circuit parameters* Working pressure: 98 kPa Hose size: DN5 *Communication* EtherCAT connector

operated by hydraulic pressure. There is a hydraulic brake integrated in the unit body. The vacuum is led through the center of the unit. The fixture unit is mounted in the housing. The hydraulic hoses are mounted on the housing. The communication electronics and the hydraulic servo-valves are mounted next to the hydraulic cylinder. The housing is custom-made and robust for ensuring stiff support of the part. The technical parameters of the fixture are summarized in Table 5.2.

In general, two types of raw parts are typically used: rigid and flexible. An aluminium block is an example of a rigid raw part. Pre-formed metal or composite sheet is an example of a flexible raw part. The unit can work in two operational
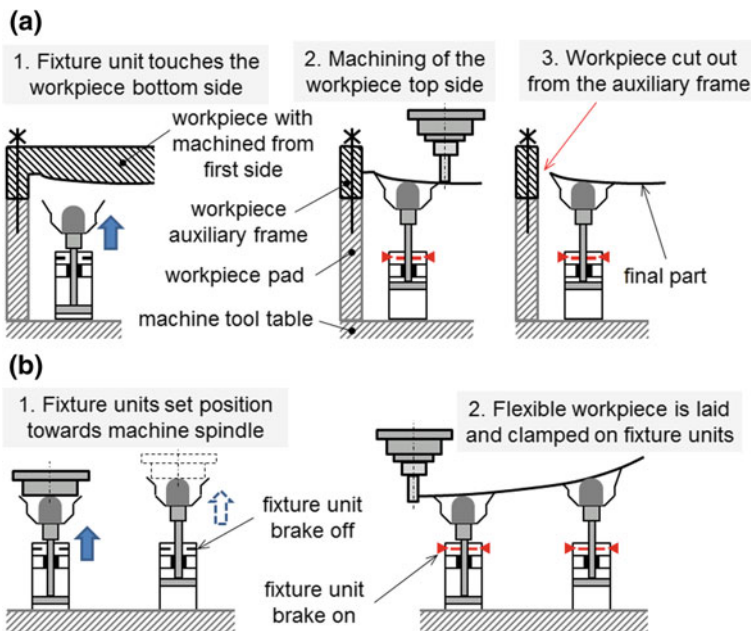

Fig. 5.6 Strategies for position setting of the support point and workpiece clamping: (a) clamping of the rigid raw part; (b) clamping of the flexible raw part

modes to be able to clamp both mentioned raw part types. The main difference is in position setting of the support point.

In case of the rigid raw part, the workpiece is clamped with standard fixtures using the auxiliary frame (Fig. 5.6a) that is an integral part of the workpiece. The positions of all fixture units are set according to the workpiece shape machined in a previous step. The fixture movement force should be very small for ensuring just a gentle touch with the raw part without its deformation. Then, the fixture position is locked by the fixture brake. The workpiece is clamped to the fixture using the vacuum cup. The top side of the part can be machined. As a last operation, the final workpiece is cut out from the auxiliary frame.

If the flexible raw part is used, the fixture can set the support points to the workpiece negative shape. Since the raw part has low stiffness, it cannot be used for setting the positions of every particular fixture unit. The fixture unit positions should be set by touching the supporting points towards the specific Z position defined by the spindle position (Fig. 5.6b). This constitutes an easy solution that reduces the fixture unit cost and that ensures the accuracy of the whole fixture in relation to the machine tool accuracy.

The clamping of the thin-walled part using the vacuum cups can cause too big workpiece deformations if an improper combination of the vacuum cup diameter, the vacuum pressure and the fixture distance is used. An approximate analytic model of the workpiece deformation due to clamping using the vacuum cups was derived for fast decisions when designing the clamping of the workpieces with increased compliance. The solution provides a relationship between the workpiece deformation and the parameters of the clamping system, such as the size of the fixture, level of vacuum and distance between the fixture units.
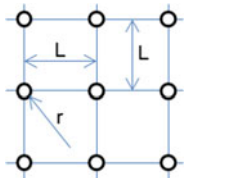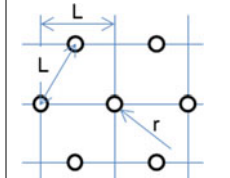
The equation was derived using the theory of thin plates. The main assumptions for the analytic model were the following: elastic behaviour of material, small rotations and deformations of the workpieces. The equation was derived for a plate of infinite width. The equation is valid only in the array between the fixture units, not outside of this array (between the fixture units and the edges of the workpiece). The deformation of the workpiece can be computed as:

$$u_{\max} = \frac{\alpha \cdot \beta}{64 \cdot D} \left[5 \cdot \rho \cdot g \cdot t \cdot \left(\frac{L}{2}\right)^4 + p \cdot \left(\frac{r}{\alpha}\right)^4 \cdot \left(5 + 4 \cdot \ln \frac{L/2}{r/\alpha}\right) \right] \qquad (5.1)$$

where:

α, β [−]	are correction coefficients (see Table 5.3),
D [N/mm]	is bending stiffness of the workpiece,
g [m/s^2]	is gravitational acceleration,
r [mm]	is radius of the fixture's vacuum cup,
L [mm]	is distance between the fixture units,
p [MPa]	is vacuum pressure in the fixture unit,
t [mm]	is plate thickness,
ρ [tonnes/mm^3]	is density of workpiece material,

Table 5.3 Correction factors for two fixture patterns

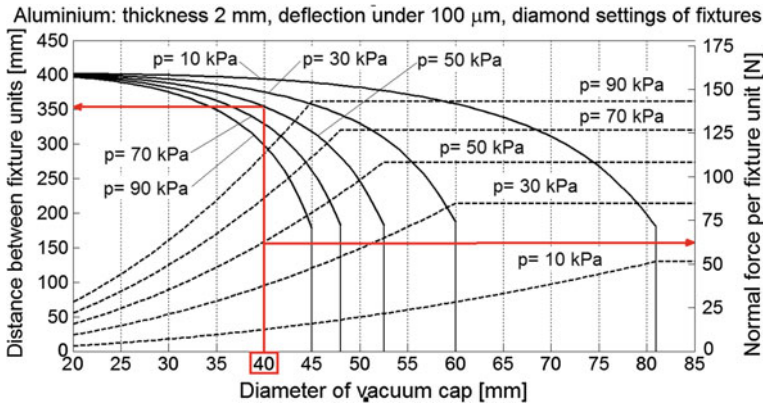|	Square pattern: $\alpha = 1.101$ $\beta = 1.076$		Diamond pattern: $\alpha = 0.961$ $\beta = 0.792$

Fig. 5.7 Example of the alignment chart for an aluminium workpiece with thickness 2 mm, requested maximum deformation under 100 μm and diamond setting of fixture units

v [−]   is Poisson constant of workpiece material,
E [N/mm^2]   is Young's modulus of workpiece material.

The bending stiffness D of the workpiece can be computed using the thickness t and Young's modulus of the material as:

$$D = \frac{E}{1 - v^2} \cdot \frac{t^3}{12} \tag{5.2}$$

It can be seen from the comparison of the correction coefficients that the diamond configuration is more efficient than the square configuration, as its usage leads to a lower deflection while needing a lower number of fixture units in the same space. The diamond configuration results in a more uniform distribution of the deformation.

The analytic model was verified using finite element analysis. The variation of the result was in the range of ±3% in the case of the square pattern and ±8% in the case of the diamond pattern. This error is acceptable for an approximate determination of the fixture point positions and clamping system parameters.

Using Eq. (5.1), graphs for various combinations of the fixture system parameters can be computed. An example of this chart is depicted in Fig. 5.7. The

diagram enables fast selection of the vacuum pressure for a specific vacuum cup diameter and a fixture unit distance. An additional information from the chart is the clamping force per fixture unit for the selected solution. Thereby, the fixture designer can quickly and easily select the clamping system configuration for a given workpiece material, workpiece wall thickness and requested precision.

The simplifications of the analytic solution do not enable to involve possible parameters of the real workpiece, such as its curvature or presence of the local reinforcements, for example ribs. The chart can still be used if the minimal wall thickness of the workpiece is chosen as the input parameter. In the case of the reinforced structures or of the curved structures, the usage of the charts, with design parameters from the flat workpieces of uniform thickness, will result in a tendency to predict lower distances than necessary, i.e. it will give safer results in terms of achieving the demanded precision. Therefore, the charts are suitable for practical application. On the other hand, the usage of charts might increase the number of fixture units in comparison to the number that would be necessary.

5.4   Thickness Sensor

Various methods for thickness measurement were analysed. Measurement methods based on ultrasound were identified as the most effective and accurate physical principle for thickness measurement of non-ferrous non-magnetic materials. There are several systems available on the market. Here, a system made by company Olympus was chosen. The Olympus 38DL Plus thickness gauge is shown with accessories in Fig. 5.8a. The accessories consist of a probe working on a frequency of 10 MHz and the RS232 cable for serial communication. The great advantage of the device is the real time communication using the RS232 interface. Other thickness gauges with RS232 interface exist; however none of them enables real time communication. The Olympus 38DL Plus allows a continuous output mode. The limitation of the serial communication is based on data transfer as a function of
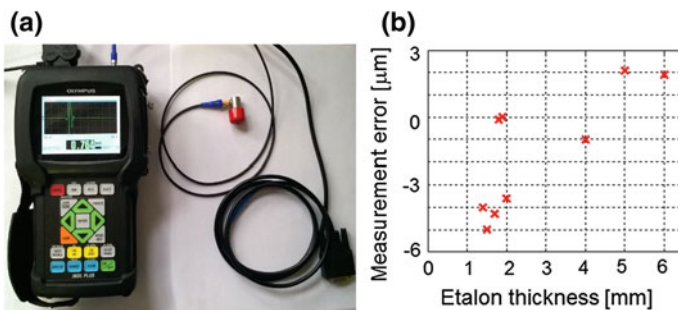

Fig. 5.8 The ultrasonic Olympus 38DL Plus thickness gauge: (a) device with accessories; (b) error of thickness measurement for different etalons

cable length. In the case of a sampling frequency $f_s = 20\,\text{Hz}$ the recommended cable length should be less than 60 m. The device can be operated using different power supplies, including both AC power and battery.

The ultrasonic thickness sensor was tested on the Johansson gauges [7]. The sampling frequency was set up to $f_s = 20\,\text{Hz}$ and 10 samples were captured. The largest gauge ($t = 6$ mm) was used for the ultrasonic velocity calibration, the smallest one ($t = 1.4$ mm) for the "zero point" calibration. The calibration has to be done for different materials and should be repeated in time in case of temperature change. The results of the measurements are shown in the graph in Fig. 5.8b. It can be concluded that the accuracy of the device in the experiment was ± 5 µm which is suitable for the requested application.

5.5   Operator Software

A specific software called LECLIN (LEveling, CLamping, INspection) with modules for workpiece inspection using a touch probe and thickness measurement using the thickness sensor was developed for easy fixture system control by the machine operator.

Positions of the measuring points for the determination of the workpiece orientation within the working area of the machine tool are indicated graphically in the software. The system can automatically calculate a workpiece local coordinate system transformation after manual measurement of all necessary points. It is possible to perform automatic inspection measurement after workpiece alignment. The workpiece inspection is fully controlled in the designed software (trajectory planning, movement control, result display) which cooperates with a Heidenhain machine tool control system very closely and online (see next section). The measurement results are shown afterwards in the software main screen. The software is also used for the control of the movement of the fixture units and for vacuum clamping.

The software may be used for an inspection of the workpiece thickness using the ultrasonic probe. Although the thickness measurement represents a special type of inspection, the principle, trajectory planning and result visualization is the same as for measurements with the touch probe.

All mentioned software functions enable the machine tool operator to control the whole fixture and inspection process easily from one place.

5.6   Communication Concept and Complete Fixture System Description

The complete intelligent fixture system consists of a group of fixture units, a thickness sensor and a central unit (industrial PC—IPC), see Fig. 5.9. The IPC controls the movement of all connected fixture units and also includes the
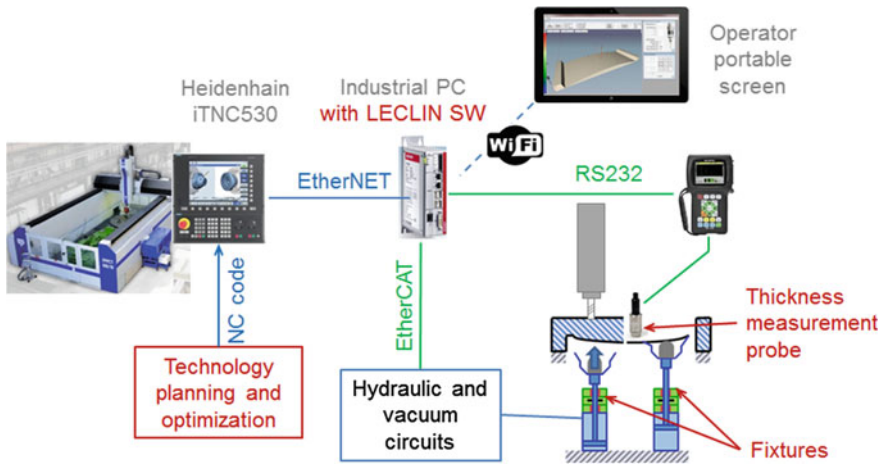
Fig. 5.9 Communication and connection scheme of the fixture system

human-machine-interface (software LECLIN) for checking, control and visualization of the fixture status. To fulfill these functions, the IPC is connected with the machine tool control system (Heidenhain iTNC530 in this case) and an operator portable screen through Ethernet. The IPC enables sharing information with the machine tool control regarding the system status, the actual position of the machine tool and the touch probe status. Concurrently, the IPC computes input values for the fixture system setting using information from the CAD representation of the workpiece. The IPC also processes measured thickness data together with the information from the machine tool control system. This solution enables the workpiece thickness inspection directly in the workspace of the machine tool. The vacuum and hydraulic actuators are centrally controlled by the IPC and its distributed input and outputs (IO) through EtherCAT. The thickness sensor is connected to the IPC and its distributed IO through serial communication.

5.7   Tool Selection and Cutting Condition Optimization

Machining stability is the key topic during the machining technology planning. In this work, there were two specific tasks: The first task was to find optimal chatter-free cutting conditions for all specific tools for high volume roughing. The second task was to find the optimal tool geometry for productive finishing operation, but minimized axial force.

An example of the chatter-free cutting conditions is given in Fig. 5.10. The stability of machining was checked with noise measurement using a microphone. The stable process conditions were evaluated by the noise spectrum analysis for
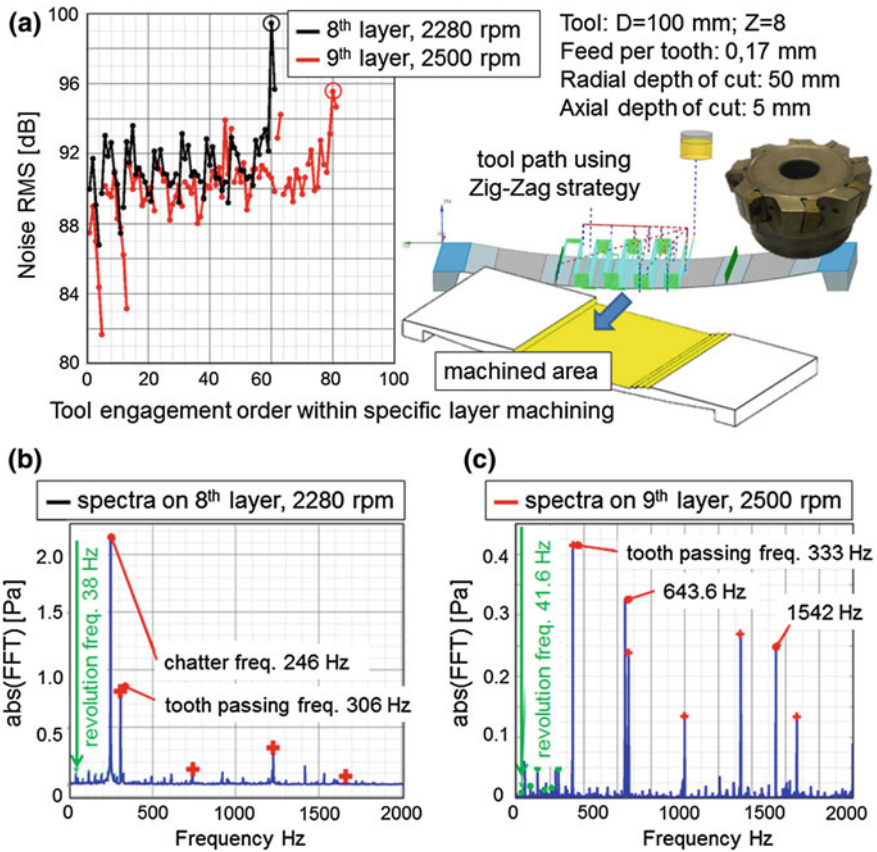
Fig. 5.10 Example of the tool revolution optimization procedure used during workpiece inner side roughing: (a) comparison of noise RMS values; (b) spectrum of the noisiest cut with 2280 rpm; (c) spectrum of the noisiest cut with 2500 rpm

operation with the highest noise RMS value (Fig. 5.10a). The workpiece roughing operation of the inner side was done layer by layer with a milling head using a zig-zag strategy. The layer thickness was 5 mm. A chatter frequency of 246 Hz was detected within machining of the 8th layer (Fig. 5.10b), thus the tool revolutions had to be changed.

Chatter arises due to dynamic forces. These forces are generated by cutting of a wavy workpiece surface with a vibrating tool. There must be a non-zero phase shift between the vibrating tool and the wavy surface [3]. The phase shift ψ can be computed for specific tool revolutions and a specific chatter frequency using Eq. (5.3). For zero dynamic force, the phase shift ψ must be equal to zero.

$$\frac{60 \cdot f_{chatter}(\text{RPM}_{tool})}{RPM_{tool}} = \text{integer} + \frac{\psi}{2\pi} \tag{5.3}$$

The identified chatter frequency is uneven order of the revolution frequency:

$$\frac{60 \cdot 246}{2280} = 6.47 \tag{5.4}$$

In order to determine new tool revolution speeds, the value on the right side of the equation must be an integer:

$$\frac{60 \cdot 246}{6} = 2460\,\text{rpm}; \quad \frac{60 \cdot 246}{7} = 2108\,\text{rpm} \tag{5.5}$$

It is better to use higher tool revolutions for higher machining productivity. Since the chatter frequency of 246 Hz is higher than the frequency related to the relevant eigenmode identified by the measured FRF on the workpiece, the potentially higher chatter frequency could be expected with increased tool revolutions. In order to ensure zero dynamic force by the phase shift (5.3), the tool revolutions were set to 2500 rpm which is slightly higher than the computed revolutions of 2460 rpm (5.5).

The machining of the 9th layer with the new value of the tool revolution was stable compared to the previous case (Fig. 5.10c). The highest peak in the spectrum is the tooth passing frequency which indicates stable cutting. The described procedure was used for an optimization of all critical cutting conditions during preliminary machining tests. The optimized revolution values enabled stable cutting in all workpiece layers, therefore the axial depth of cut of 5 mm was not decreased in any layer.

Three cutting tool geometries were tested for finishing operations in order to find an appropriate compromise between productivity (larger tool tip radius = higher productivity at specific scallop size) and chatter limits (larger tool tip radius → higher axial cutting force → higher risk of chatter occurrence and higher static deformation of the workpiece). The following three tool geometries were used: monolithic cutter with a tip radius of 20 mm; toroidal cutter with round tips with a radius of 8 mm; cutter with changeable tips with a radius of 3 mm (Fig. 5.11b). The vibration signal was obtained using a microphone (Fig. 5.11a). The surface quality was also compared for all three tools (Fig. 5.11c). The tool with changeable tips with a corner radius of 3 mm was used for final machining of the demonstration part. The high tool revolution speed together with a small cutting contact zone of the 3 mm tool tip radius and tool tilt angle generated a low dynamic cutting force and subsequently also the stable cut.
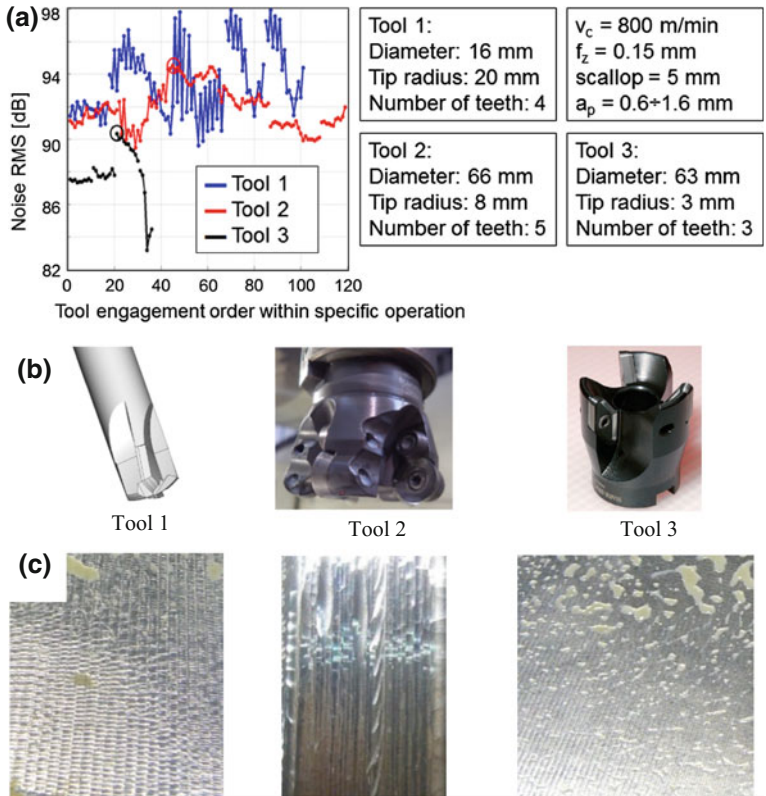
Fig. 5.11 The tested tools for finishing operation: (a) comparison of noise RMS values; (b) tool geometries; (c) final workpiece surfaces

5.8 Overall Machining Strategy

The final workpiece deformation of the thin-walled workpiece consists of partial deformations. Some of these workpiece deformations are predictable using mathematical models (e.g. static deformation due to cutting force load or clamping force load); some of these are unpredictable (e.g. deformations due to residual stress). Adaptive machining technology involving the inspection of the current state of the workpiece geometry seems to be suitable for effective finish machining. The machining approach was developed and verified for productive machining with high demands on final workpiece accuracy.

The main machining steps are summarized in the following. Please note that the procedure describes machining of the workpiece inner surface, i.e. top surface during the second machining step. The workpiece outer surface is the bottom surface during this phase of machining.
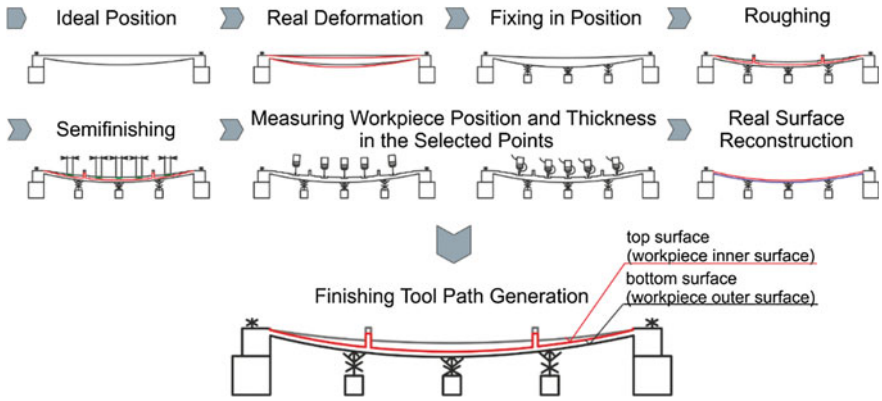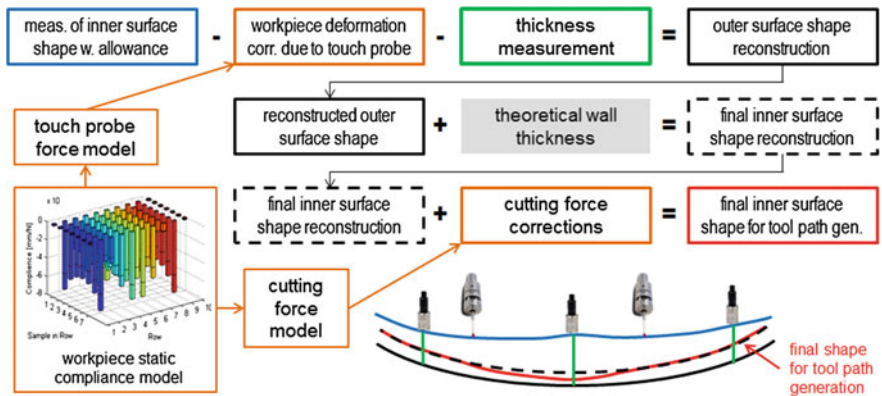
Fig. 5.12 Machining process overview

Fig. 5.13 Reconstruction of the substitutive surface for part finishing

The process starts with machining of the first (outer) side of the workpiece. It is conventional machining of a thick-walled stiff workpiece without any special issues. Then, the workpiece is turned around and clamped using the auxiliary frame and the additional fixture units with the vacuum cups (Fig. 5.12). A proposal of the number and position (pattern) of vacuum fixture units is elaborated for improving the workpiece stiffness. Suitable machining conditions are proposed and the tool path is generated for roughing and semi-finishing operation.

The adaptive machining technology is used for finishing of the part (Figs. 5.12 and 5.13). It involves an inspection of the current state of the workpiece geometry. The main goal is to gain information about the top and bottom surface shape and to create a substitutive surface for tool path generation for a correction of the wall thickness during the last machining operation.

The workpiece current state is inspected by a touch probe for real surface position identification in selected points (Fig. 5.14a). The workpiece deformation caused by the touch probe has to be compensated because of the high compliance of
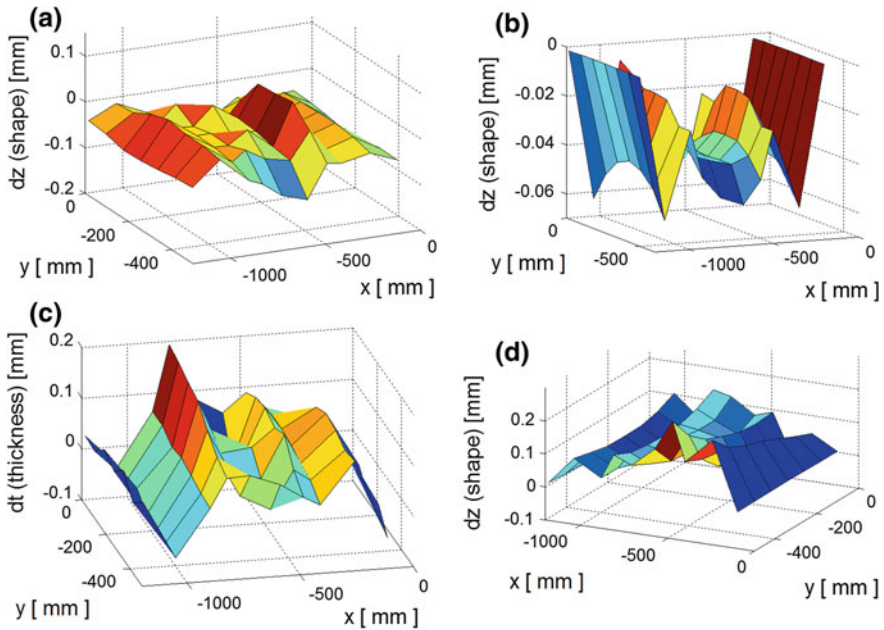
Fig. 5.14 Measured information about shape and thickness of the workpiece: (a) measured inner (*top*) surface shape; (b) workpiece deformation due to touch probe; (c) thickness deviation of finished workpiece with stiffness correction obtained from top surface deviation; (d) final inner surface shape for tool path generation using machining force and workpiece stiffness compensation

the workpiece and the high stiffness of the probe (Fig. 5.14b). The thickness of the workpiece is measured by an ultrasonic probe in the same selected points where the identification with the touch probe was done (Fig. 5.14c). The real bottom (outer) surface of the workpiece is reconstructed from the information about the top surface and the real wall thickness. The new theoretical top (inner) surface is generated using information about the real bottom surface and the theoretical thickness. This surface shape is corrected with respect to the cutting force model and the simulated workpiece compliance (Fig. 5.14d). The NC code for the finishing operation is generated using this corrected surface shape.

5.9 Case Study Results

The workpiece thickness was evaluated at 70 points. The chart of the thickness error is presented in Fig. 5.15. The wall thickness was below the lower tolerance in two cases and above the upper tolerance in 32 points. The maximum thickness error is ± 0.1 mm. For comparison: if the machining process is done without the in-process workpiece inspection, the final thickness error reached a value of 0.9 mm.
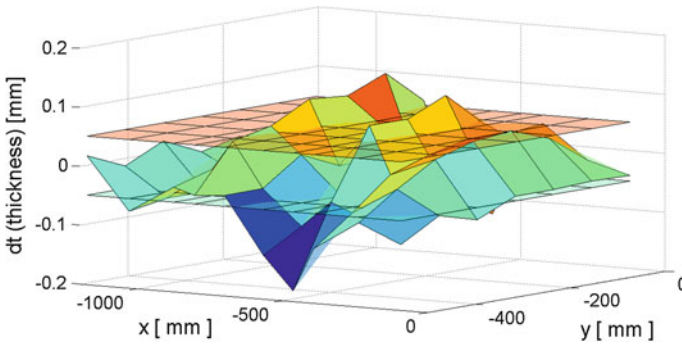
Fig. 5.15 Thickness measurement results

Table 5.4 Results compared with key performance indicators

Parameter	Requirements	Previous technology	Developed solution	Status
Workpiece wall thickness tolerance	±0.05 mm	±0.1 mm	±0.1 mm	Partially better
Workpiece weight tolerance	Max. +1 kg	+2 kg	+1 kg	Ok
Surface roughness	Ra 0.8	Ra 0.8	Ra 0.8	Ok
Machining time of the inner side	To minimize	100 h	85.1 h[a]	−15%
Price	To minimize	EUR 130,000[c]	EUR 95,000[b]	−27%

[a]Simulation result using the experimentally verified parameters
[b]Price of the full fixture set; the set includes six specific fixture devices for six main parts of the airplane wing
[c]Price of the universal fixture device based on the developed fixture units and control software

5.10   Case Study Summary

The main KPIs are compared in Table 5.4 with the results obtained on the demonstration part and applied to the full-sized part using a simulation. As can be seen, the proposed manufacturing procedure enables an improvement of the main manufacturing indicators compared to the results of the existing industrial solution.

The proposed manufacturing procedure is beneficial from the productivity point of view: The proposed manufacturing process leads to a shortening of the production time (of the inner surface) by about 15% with the requested quality of *Ra* = 0.8. The proposed manufacturing procedure is acceptable from the accuracy and weight point of view: The wall thickness is below the lower limit only in two points at the part margin. Since the value stayed within 2T (double tolerance) zone, the strength of the final part should not be affected. The wall thickness is above the

upper limit at some points. Thus, the total weight should be evaluated in order to fulfill the requirements. The part weight is on the requested upper limit.

The proposed fixture system is cost-effective: The proposed universal solution has a lower price compared to the total price of the existing dedicated fixture set. A group of fixture units, including the necessary harness and control, offers a universal possibility how to replace a set of six specific fixtures designed as a mold with the negative shape of the part. Moreover, the new fixtures can be used for clamping during machining of both workpiece sides. The key financial benefit is the ability to replace more types of specialized clamping devices.

5.11   Conclusions

Production of thin-walled curved workpieces is difficult due to the low static and dynamic stiffness of the workpiece. The principle approach presented in this case study is based on a workpiece clamping using discrete fixture units, machining strategy optimization with respect to the part properties and adaptive machining technology involving the inspection of the current state of the workpiece geometry. As the results of the study showed, this solution is cost-effective and enables productive and accurate machining. The main advantage of the solution is the universal application of the developed fixture units and the automatic process control including part thickness measurement.

References

1. Böhm Feinmechanik, Vacuum clamping devices. (2016) Available on-line: http://www.boehm-feinmechanik.com/html/vacuum_clamping_devices.html
2. Tobias, S.A., Fishwisck, W.A.: Theory of Regenerative Chatter. The Engineer, London (1958)
3. Tlusty, J., Polacek, M.: The stability of machine tool against self-excited vibrations in machining. In: Proceedings of the International Production Engineering Research Conference: 465–474, Carnegie Institute of Technology, Pittsburgh, Pennsylvania (1963)
4. Budak, E.: Mechanics and dynamics of milling thin walled structures. Ph.D. Thesis, University of British Columbia (1994)
5. Davies, M.A., Balachandran, B.: Impact dynamics in milling of thin walled structures. Nonlinear Dyn. **22**(4), 375–392 (2000)
6. Herranz, S., Campa, F.J., Lopez de Lacalle, L.N., Rivero, A., Lamikiz, A., Ukar, E., Sanchez, J.A., Bravo, U.: The milling of airframe components with low rigidity: a general approach to avoid static and dynamic problems. Prod Institution Mechanical Eng. Part B. J. Eng. Manuf. **219**(11), 789–801 (2005)
7. Gauge block. (2016). Available on-line: https://en.wikipedia.org/wiki/Gauge_block